APPLIED GEOPHYSICS, Vol.12, No.2 (June 2015), P. 212-220, 10 Figures.
DOI: 10.1007/s11770-015-0484-2

Low-frequency data analysis and expansion*

Zhang Jun-Hua♦[1], Zhang Bin-Bin[1], Zhang Zai-Jin[1], Liang Hong-Xian[2], and Ge Da-Ming[2]

Abstract: The use of low-frequency seismic data improves the seismic resolution, and the imaging and inversion quality. Furthermore, low-frequency data are applied in hydrocarbon exploration; thus, we need to better use low-frequency data. In seismic wavelets, the loss of low-frequency data decreases the main lobe amplitude and increases the first side lobe amplitude and results in the periodic shocking attenuation of the secondary side lobe. The loss of low frequencies likely produces pseudo-events and the false appearance of higher resolution. We use models to examine the removal of low-frequency data in seismic data processing. The results suggest that the removal of low frequencies create distortions, especially for steep structures and thin layers. We also perform low-frequency expansion using compressed sensing and sparse constraints and develop the corresponding module. Finally, we apply the proposed method to real common image point gathers with good results.
Keywords: seismic wavelet, forward modeling, low-frequency expansion, compressed sensing, sparse constraint

Introduction

To improve the resolution in seismic exploration data, much attention was paid to high-frequency data; nevertheless, geophysicists gradually understood the importance of low-frequency signals (ten Kroode et al., 2013). In addition to improving inversion accuracy, there are many advantages in using low-frequency data (Baeten et al., 2013). First, low-frequency data can reduce the amplitude of side lobes in wavelets and improve the seismic vertical resolution (Kallweit and Wood, 1982). Second, in seismic wave propagation, low-frequency data have stronger penetration and anti-absorption than high-frequency data; therefore, the image quality of complex structures is improved (Ziolkowski et al., 2003; Woodburn et al., 2011). Third, in oil and gas exploration, we can use low-frequency seismic shadows to locate hydrocarbons (Castagna et al., 2003; Chen et al., 2012). Fourth, when using low-frequency data, the number of local minima in least squares misfit functions used in full-waveform inversion is smaller; thus, convergence to global minima improves (Sirgue and Pratt, 2004; Kelly et al., 2009).

To acquire low-frequency data, we need to consider the seismic source and acquisition technology. Presently, there are significant developments in low-frequency data acquisition. The lowest acquired frequency is about 3 Hz (Tao et al., 2011) and the lowest receiver frequency is 2 Hz (Sun et al., 2012; Li et al., 2013). However, the

Manuscript received by the Editor January 30, 2015; revised manuscript received April 27, 2015
*This work was supported by the National Science and Technology Major Project (No. 2011ZX05051) and Science and Technology Project of Shengli Oilfield (No. YKW1301).
1. School of Geosciences, China University of Petroleum (East China), Qingdao 266580, China.
2. Geophysical Prospecting Research Institute of Shengli Oilfield, Dongying 257022, China.
♦Corresponding author: Zhang Jun-Hua (Email: zjh_upc@163.com)

cost of low-frequency data acquisition is significant. In China, conventional seismic acquisition methods in seismic exploration use 5 Hz for the source and 10 Hz for the receiver; that is, seismic data with frequency lower than 10 Hz are strongly affected by noise. Moreover, the suppression of surface waves also affects the low-frequency components. Thus, researchers at home and abroad have looked at improving the low-frequency data processing methods (e.g., Guan and Tang, 1990; Whitcombe and Hodgson, 2007; Woodburn et al., 2011). Nevertheless, the currently available low-frequency processing methods have many limitations, e.g., strong interference in the low-velocity zone influences the effect of low-frequency expansion; the low-frequency stabilization based on spatial filtering only operates on low-frequency slices; the significance of frequency compensation is not clear; low-frequency expansion based on the deconvolution operator only processes the wavelet and not considering the wavelet change of the formation. In this study, we apply compressed sensing theory to real seismic data. Compressed sensing was proposed by Candès et al. (2006a, 2006b) and Donoho (2006). They pointed out that the original signal can be reconstructed by using the optimal sparse reconstruction algorithm based on the signal sparse prior information, and the signal of the adaptive linear projection for sampling far below the Nyquist frequency. In signal reconstruction, we generally obtain the solution using sparse constraints (Yuan et al., 2015; Han et al., 2012). Presently, compressed sensing has been used in seismic data recovery (Herrmann et al., 2006; Bai et al., 2014), plane wave decomposition (Wang and Wang, 2014), and other cases.

Although much work has been done regarding low-frequency seismic data, and their importance in oil and gas exploration has been recognized, the necessary quantitative analysis is lacking. We analyze the characteristics of seismic wavelets, synthetic seismograms, and models of geological structures with and without the use of low-frequency data. At the same time, the low-frequency data was expanded based on the theory of compressed sensing. Low-frequency energy is obviously enhanced after applying the method and the structure information is richer.

Low-frequency seismic data analysis

According to the seismic convolution model, the amplitude of seismic data depends on the convolution of the wavelet and reflection coefficient. Therefore, we discuss the loss of low-frequency seismic data in the source wavelet, seismic data, and geological models and analyze the results.

Single seismogram

First, we analyze the loss of low-frequency data in a wavelet because the wavelet spectrum strongly affects the seismic record. We use a 30 Hz Ricker wavelet, 2 ms sampling interval, and 101 sampling points. We use low-cut filters of 4 Hz, 8 Hz, and 12 Hz in the frequency domain. The waveform comparison is shown in Figure 1.

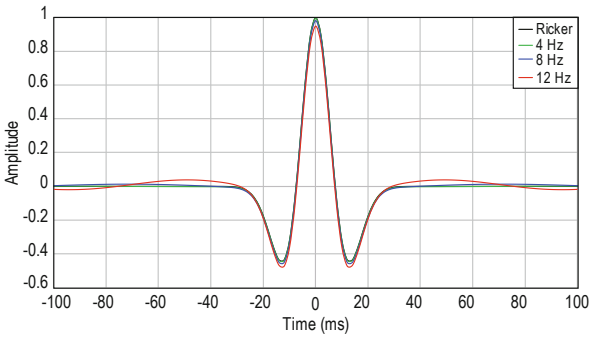

Fig.1 Wavelet with different low-cut frequency filters.

Figure 1 shows that the loss of low-frequency data decreases the main lobe amplitude, increases the first side lobe amplitude, and increases the secondary side lobe amplitude of the periodic oscillation. With increasing removal of low-frequency components, the oscillation period of the wavelet decreases and the amplitude increases.

The wavelet waveform affects the waveform of the seismic data. Thus, we design a reflection coefficient model with 150 sampling points and sampling interval of 2 ms. Then, we use reflection coefficients of 0.5, 0.4, and 0.4 that correspond to 80 ms, 200 ms, and 250 ms to convolute the reflection coefficient model using a standard Ricker wavelet and neglecting frequency data below 4 Hz, 8 Hz, and 12 Hz. Finally, we observe the differences in the synthetic seismogram, as shown in Figure 2.

We can see the secondary lobe in the seismic wavelet produces pseudo-events and amplitude distortion. For example, the side lobe amplitude changes at the red arrows. The lack of low-frequency data can lead to waveform changes in the time domain and this will affect the fine-scale description of reservoirs and hydrocarbon detection.

Geological models

The spectrum of the reflection coefficient affects

the spectrum of the seismic data; thus, we design a series of different geological models and analyze the characteristics of losing low-frequency components in a thin-layer, an anticlinal pinch-out, and a structurally complex geological model.

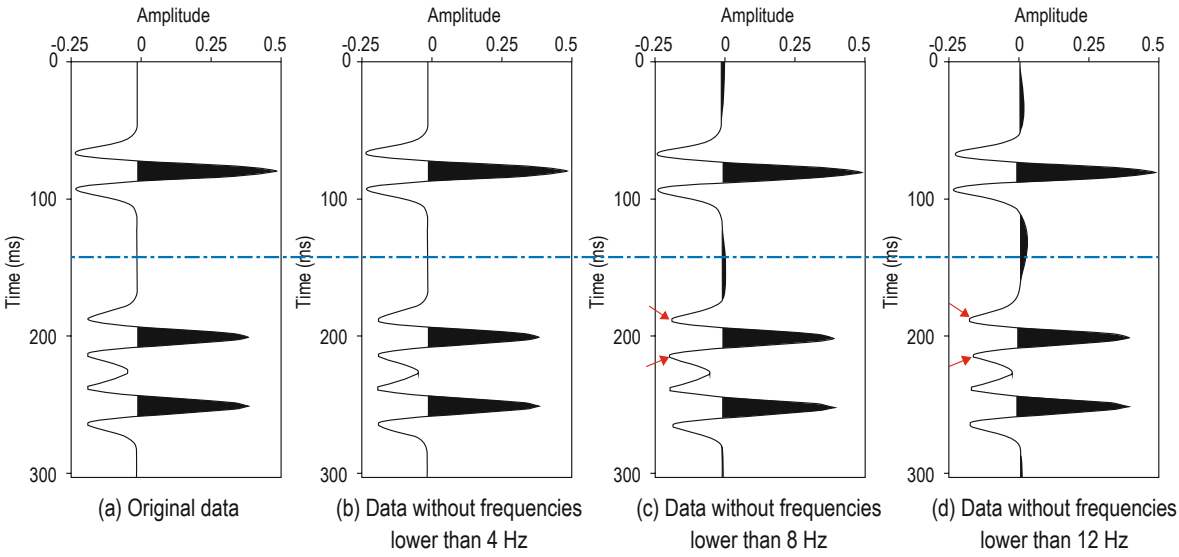

Fig.2 Synthetic seismograms.

1. Thin-layer model

We design a thin-layer model (Figure 3) and then filter out the low-frequency data using the same parameters as above.

As shown in Figure 3, the removal of low-frequency data causes the distortion of small events in the thin layer and the appearance of pseudo-events in the data without frequencies less than 8 Hz. This will certainly affect the layer detection; furthermore, the above observations are consistent with the characteristics of the synthetic seismogram without low-frequency data.

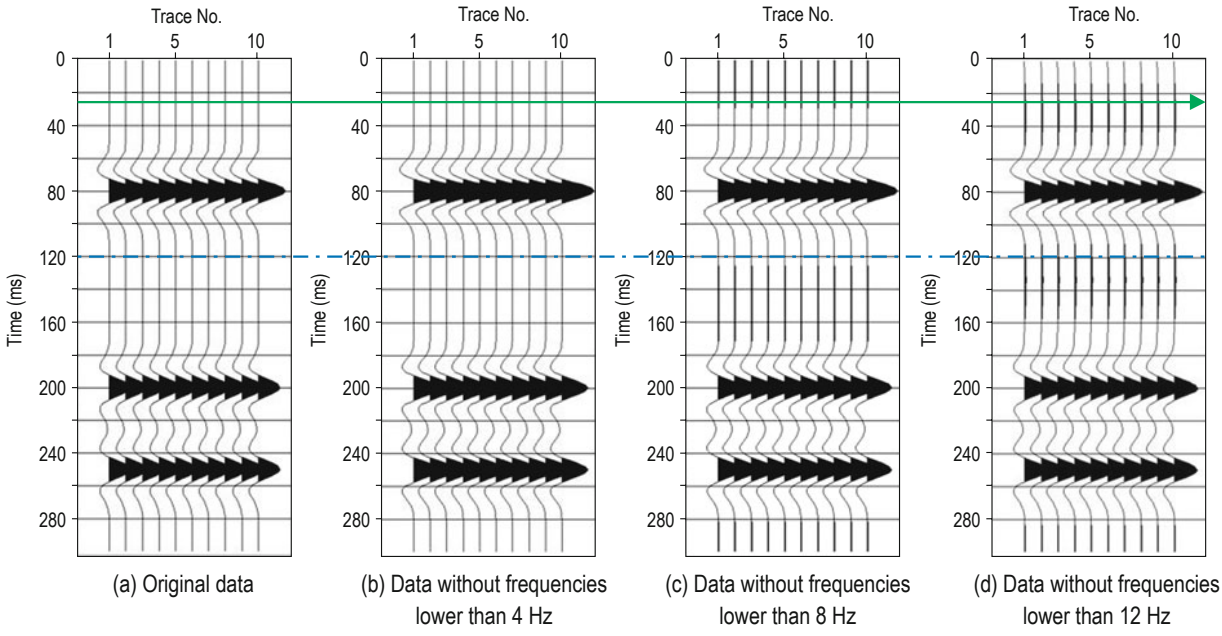

Fig.3 Thin-layer model with and without low-frequency data.

2. Anticlinal pinch-out model

We design an anticlinal pinch-out model (Figure 4) and filter out the low-frequency data using the same parameters as above. Then, we analyze the F–X spectrum of the original data (Figure 4), and we show the time-domain data containing 0–4 Hz, 0–8 Hz, and 0–12 Hz low-frequency components (Figure 5).

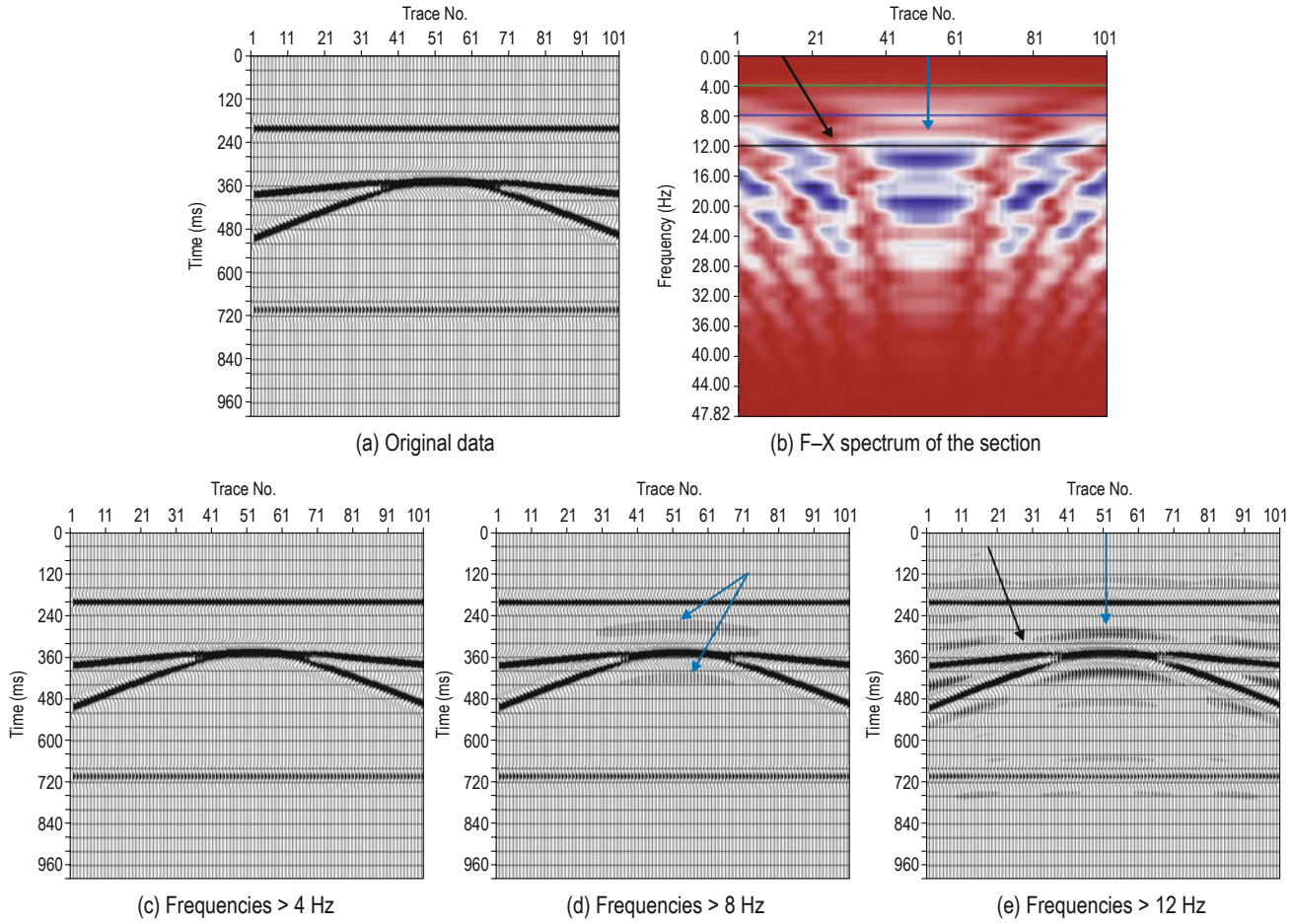

Fig.4 Anticlinal pinch-out model without low-frequency data and corresponding F–X spectrum.

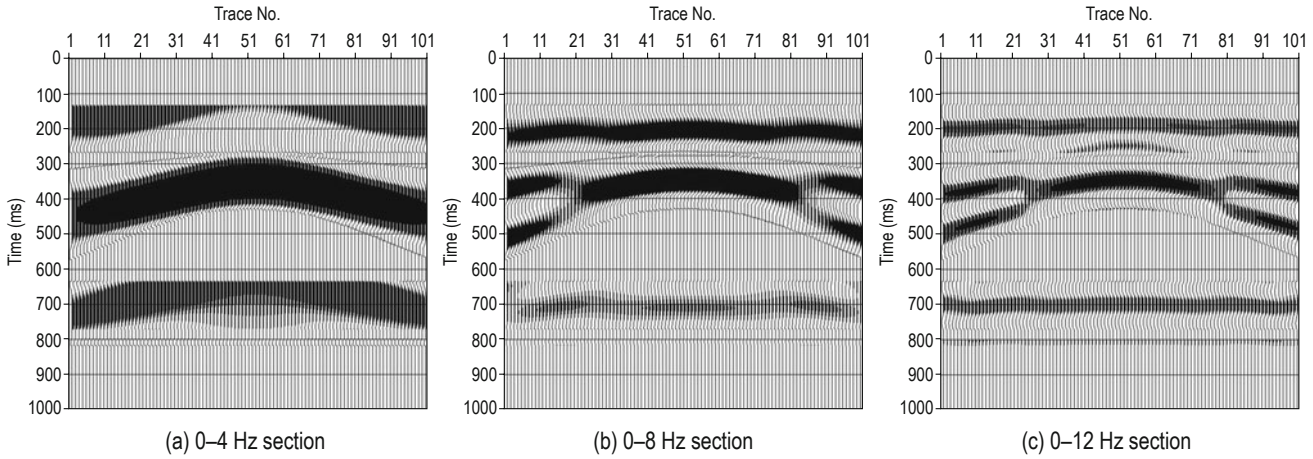

Fig.5 Anticlinal pinch-out model only with low-frequency information.

Figures 4 and 5 show that the lack of low-frequency data mainly affects the structural information. In addition, the F–X spectrum is an effective method to observe low-frequency components and lateral variation.

Finally, the main frequency of the wavelet affects the low frequency of the model. When the main frequency is low, the effect of low-frequency loss increases.

3. Structurally complex model

In order to discuss the role of the low-frequency data in inversion, we use the model in Figure 6a, which includes an anticlinal trap, a fault, and thin layers. We use a 30 Hz Ricker wavelet to do forward modeling and filter out the data with frequencies below 12 Hz. Using the velocity and density data of the model, we design seven simulation wells, and each well has an acoustic and density curve. Then, we apply wave impedance inversion using the full frequency bandwidth and remove the low-frequency data (below 12 Hz). The results are shown in Figures 6b and 6c, respectively. The comparison suggests that the loss of low-frequency data affects the inversion accuracy.

Figure 6 shows that the exclusion of low-frequency data produces results that cannot accurately reflect the variations in the various lithological and structural components of the model.

Low-frequency expansion based on compressed sensing

Compressed sensing

Let us assume that the length of the signal f is N and it can be expressed as (Donoho, 2006; Candès et al., 2006a, 2006b)

$$f = \sum_{i=1}^{N} x_i \psi_i = \mathbf{\Psi x}, \qquad (1)$$

where $\psi_i \in \mathbf{\Psi}$, $\mathbf{\Psi} \in \mathbf{C}^{N\times N}$ are matrices, and $\mathbf{x} = [x_1, x_2, \ldots, x_N]^T$ is the transform coefficients vector. If the number of nonzero elements is K and $K << N$, then f is sparse in $\mathbf{\Psi}$. We use compressed sensing to design the observation matrix $\mathbf{\Phi}$ that is not correlated with the sparse basic matrix $\mathbf{\Psi}$, and then compress and sample the signal

$$\mathbf{y} = \mathbf{\Phi} f = \mathbf{\Phi\Psi x}. \qquad (2)$$

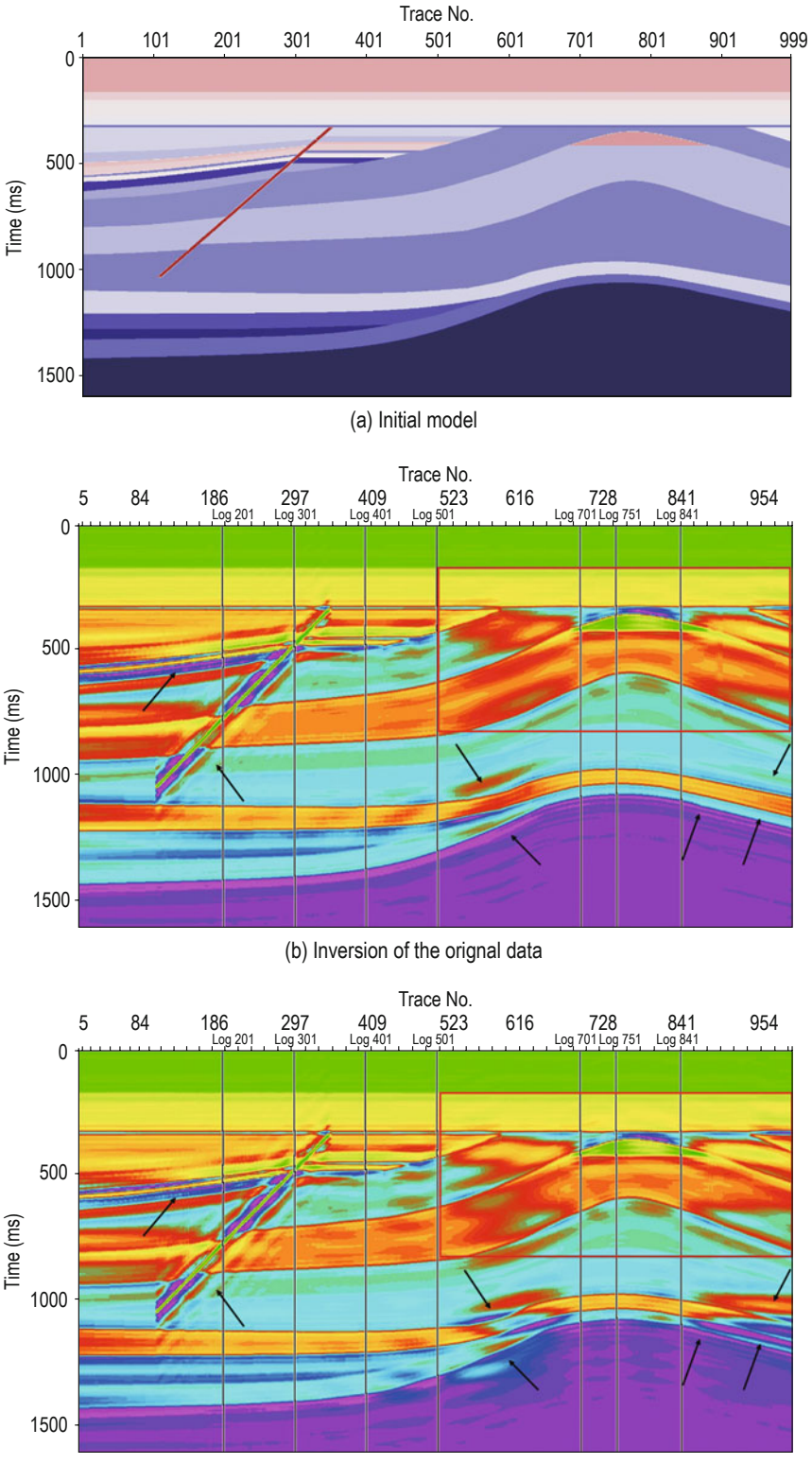

Fig.6 Inversion of the complex geological model.

Based on the sparsity of vector **x**, we can recover **x** by using a sparse promoting algorithm

$$\min \left\|\mathbf{x}\right\|_0 \quad s.t. \quad \mathbf{y} = \mathbf{\Phi} f = \mathbf{\Phi}\mathbf{\Psi}\mathbf{x}. \tag{3}$$

Equation (3) is a nondeterministic polynomial that cannot be used to solve the sparse coefficient directly. However, it turns out that one can actually recover **x** by solving the convex algorithm

$$\min \left\|\mathbf{x}\right\|_1 \quad s.t. \quad \mathbf{y} = \mathbf{\Phi} f = \mathbf{\Phi}\mathbf{\Psi}\mathbf{x}, \tag{4}$$

where $\|\cdot\|_0$ is the l_0-norm and $\|\cdot\|_1$ is the l_1-norm.

Seismic data reconstruction for low-frequency data expansion

Based on the seismic convolution model, seismic traces in the time domain can be expressed as the convolution of the source wavelet and the underground reflection coefficient (Li and Zhang, 2004)

$$y = w * x. \tag{5}$$

We transform equation (5) to the frequency domain by using the Fourier transform

$$\mathbf{Y} = \mathbf{WX} = \mathbf{WFx}, \tag{6}$$

where y is the seismic trace, w is the source wavelet, x is the reflection coefficient, **F** is the Fourier transform operator, and **Y**, **W**, and **X** represent the frequency-domain expressions of y, w, and x.

In seismic exploration, the underground reflection coefficient is treated as random sequence with full frequency bandwidth. However, because of the filter effect of the wavelet, the high and low frequencies are lost. Compressed sensing proposes that we can recover the original sparse signal by using a sparse promoting algorithm even if the original signal is affected by noise or signal components are missing (Candès, 2006b). The reflection coefficient is sparse in the time domain. This satisfies the assumptions of compressed sensing theory for sparse signals. Therefore, we can recover the reflection coefficient using compressed sensing from the seismic data that have lost the low-frequency components. We establish the minimum l_1-norm reconstruction model by using the sparse transform and solve the underdetermined problem by using a fast iterative shrinkage-thresholding algorithm to minimize

$$\min_{\mathbf{x}} \frac{1}{2}\left\|\mathbf{Y} - \mathbf{FWx}\right\|_2^2 + \lambda\left\|\mathbf{x}\right\|_1, \tag{7}$$

where $\|\cdot\|_2^2$ is the l_2-norm, **F** is the sparse matrix, **W** is observation matrix, and λ is the Lagrangian operator. First, we constrain the minimization for continuous convergence in the frequency spectrum of the seismic data by the l_2-norm. Second, we use a sparse promoting method to obtain **x** by the l_1-norm. The formula can be solved by the fast iterative shrinkage-thresholding algorithm (Beck, 2009).

We recover the seismic reflection coefficient $\hat{x}$ using compressed sensing theory and bandwidth-limited seismic data. We reconstruct the low-frequency seismic data using the low-frequency information of the reflection coefficient as follows:

$$\hat{\mathbf{y}} = \mathbf{F}^{-1}[ML(\hat{\mathbf{X}}) + MH(\mathbf{Y})], \tag{8}$$

where *ML* and *MH* are the operators for extracting the low and high frequencies after matching the amplitude spectrum of the reflection coefficient and the seismic data, $\mathbf{F}^{-1}$ is inverse Fourier transform operator, $\hat{\mathbf{y}}$ are the seismic data after low-frequency expansion.

Model data analysis

First, we set up the parameters of the reflection coefficient model. The sampling points are 201, the sampling rate is 2 ms, and the reflection coefficient is 0.8, −0.6, and 0.4 at 100, 200, and 300, respectively. Synthetic data (green line in Figure 7a) are generated by convolving a 30 Hz Ricker wavelet. The main frequency and sampling points of the wavelet are consistent with the above discussion. Then, the method is used to extend the frequency spectrum, and the results are denoted with the red line in Figure 7a. Finally, we analyze the frequency spectrum of the original and processed trace, and show the results in Figure 7b.

Figure 7b shows the frequency spectrum of the original and processed trace, which is obtained by extending the low-frequency information with the proposed method. Clearly, the low frequency is expanded and the frequency band is broadened. Figure 7a shows that the space position of the seismic synthetic trace does not change, the energy of the main lobe increases, the energy of the side lobe decreases, and the resolution improves. In conclusion, the proposed method expands the low-frequency components successfully.

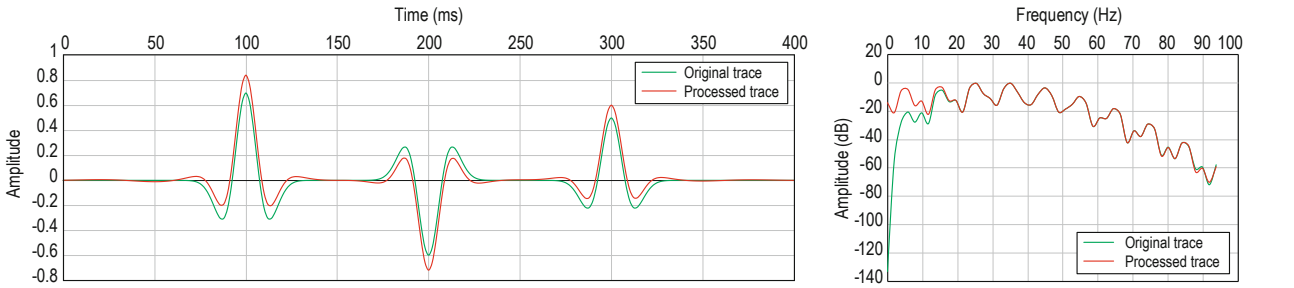

(a) Waveform before and after extension (b) Frequency spectrum before and after the extension

Fig.7 Original and processed traces.

Field data application and analysis

We apply the method on a common image point (CIP) gather and expand the low-frequency data. The comparison of the frequency spectrum of the original field and processed data is shown in Figure 8.

Figure 8 shows that the low-frequency energy of the processed data increases and the effective frequency band broadens. Owing to the limited expansion energy of the low-frequency data, the changes are not obvious in the CIP gather. Thus, we show the results after filtering (0 –10 Hz) in Figure 9.

Figure 9 shows that after the low-frequency expansion, the events extend to the near offset and the energy is obviously enhanced, which suggests that the CIP gather quality has improved and the low-frequency expansion is successful. Then, we stack the CIP gather to obtain a poststack section and show the stacked section after filtering (0–10 Hz) in Figure 10.

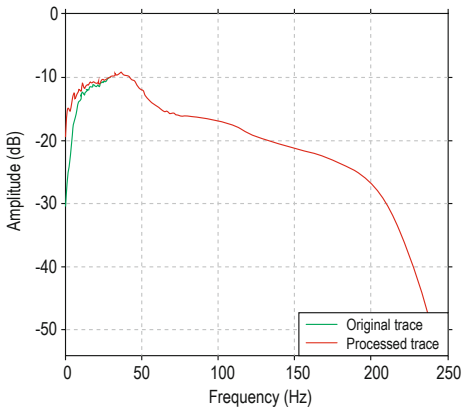

Fig.8 Frequency spectrum of the original field and processed data.

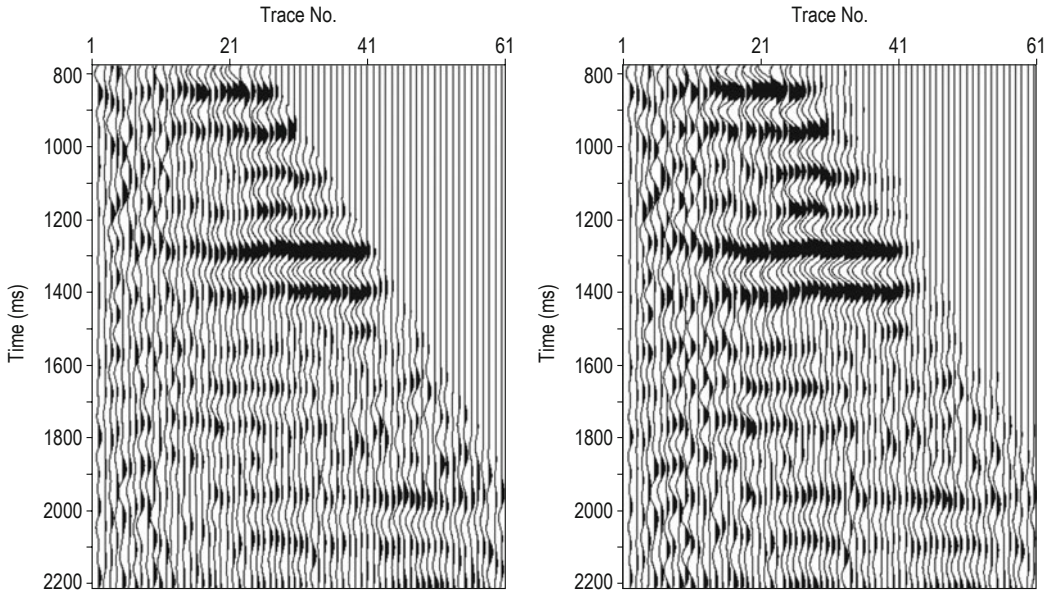

(a) Original data (b) Processed data

Fig.9 Comparison of the 0–10 Hz section using the proposed method.

Figure 10 shows that the energy is enhanced, and the fault and the breakpoints are more clear. Moreover, the basic geological features are better reflected after low-frequency expansion.

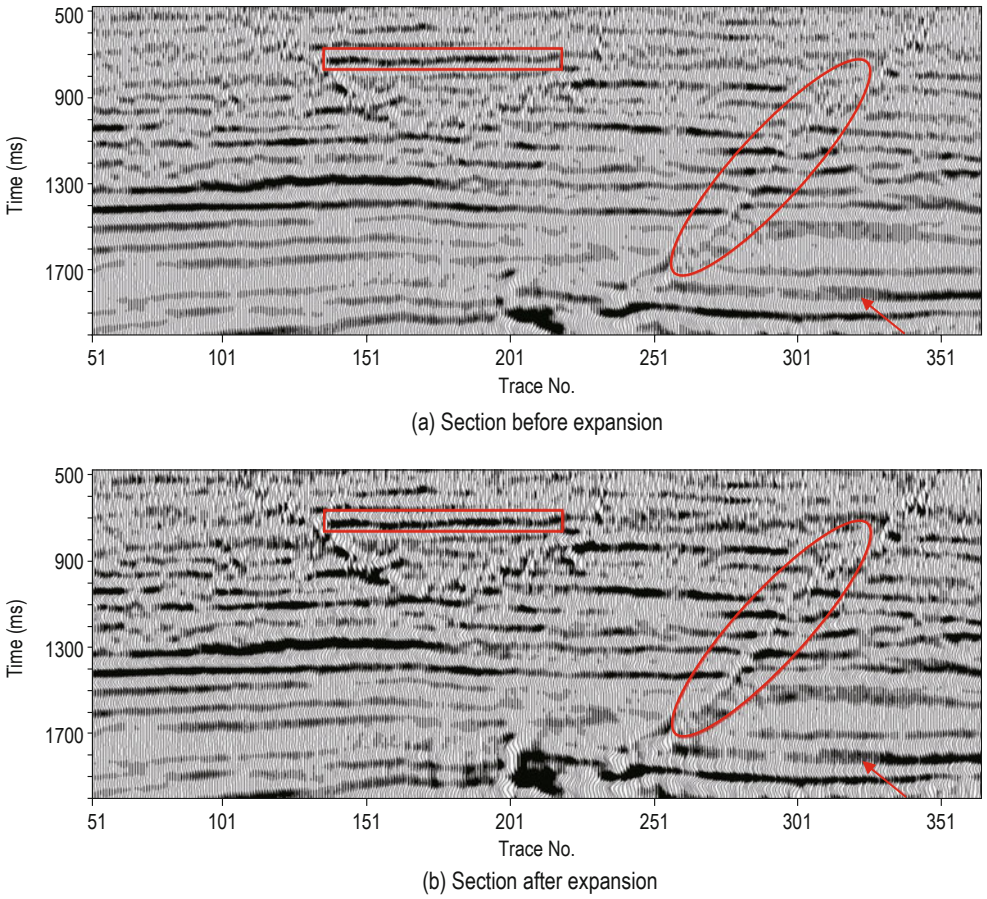

Fig.10 Stack section (0−10 Hz) before and after low-frequency expansion.

Conclusions

From the above, we can infer the following conclusions. First, in a wavelet without low-frequency data, the main lobe amplitude decreases, the first side lobe amplitude increases, and the secondary side lobe amplitude increases. The greater the low-frequency loss, the larger the secondary side lobe amplitude increase is. The wavelet strongly affects the seismic data. Hence, to obtain high-quality seismic data, we should stimulate the wavelet with low-frequency data. Second, owing to the lack of low-frequency data, the synthetic seismograms show phase distortion locally as well as pseudo-events; however, the resolution has improved. Hence, for high-resolution seismic data, we need to expand the frequency bandwidth and consider low frequencies as well. Third, F-X spectrum is a useful method to understand the lateral response characteristics when the seismic data lacks low frequency component. Four, wave impedance inversion confirms that data processing without low-frequency information cannot reflect stratigraphic and lithological variations. Therefore, in seismic data acquisition and processing, we should protect the low-frequency information and proceed with low-frequency expansion to improve the quality of seismic data. Finally, the proposed low-frequency expansion method, which is based on compressed sensing, uses the low-frequency components of the reflection coefficient to rebuild the low-frequency information in the seismic data. The proposed method clearly improves the q uality of seismic data for the inversion and interpretation.

References

Beck, A., and Teboulle, M., 2009, A fast iterative shrinkage-

thresholding algorithm for linear inverse problems: SIAM Journal on Imaging Sciences, **2**(1), 183−202.

Baeten, G., de Maag, J. W., Plessix, R. E., Klaassen, R., Qureshi, T., Kleemeyer, M., ten Kroode, F., and Zhang R. J., 2013, The use of low frequencies in a full-waveform inversion and impedance inversion land seismic case study: Geophysical Prospecting, **61**(4), 701−711.

Bai, L. S., Liu, Y. K., Lu, H. Y., Wang, Y, B., and Chang X., 2014, Curvelet-domain joint iterative seismic data reconstruction based on compressed sensing: Chinese J. Geophys. (in Chinese), **57**(9), 2937−2945.

Castagna, J. P., Sun, S. J., and Siegfried, R. W., 2003, Instantaneous spectral analysis: Detection of low-frequency shadows associated with hydrocarbons: The Leading Edge, **22**(2), 120−127.

Candès, E. J., Romberg, J. K., and Tao, T., 2006a, Stable signal recovery from incomplete and inaccurate measurements: Communications on Pure and Applied Mathematics, **59**(8), 1207−1223.

Candès, E. J., Romberg, J., and Tao, T., 2006b, Robust uncertainty principles: Exact signal reconstruction from highly incomplete frequency information: IEEE transaction on information theory, **52**(2), 489−509.

Chen, X. H., He, Z. H., Zhu, S. X., Liu, W., and Zhong W. L., 2012, Seismic low-frequency-based calculation of reservoir fluid mobility and its applications: Applied Geophysics, **9**(3), 326−332.

Donoho, D. L., 2006, Compressed sensing: IEEE Transactions on Information Theory, **52**(4), 1289−1306.

Guan, L. P., and Tang, Q. J., 1990, High/low frequency compensation of seismic signal: Geophysical Prospecting for Petroleum, **29**(3), 35−45.

Han, L. G., Zhang, Y., Han, L., and Yu, Q. L., 2012, Compressed sensing and sparse inversion based low-frequency information compensation of seismic data: Journal of JiLin University (Earth Science Edition), **42**(3), 259−264.

Herrmann, F. J., and Hennenfent, G., 2008, Non-parametric seismic data recovery with curvelet frames: Geophysical Journal International, **173**(1), 233−248.

Kallweit, R. S., and Wood, L. C., 1982, The limits of resolution of zero-phase wavelets: Geophysics, **47**(7), 1035−1046.

Kelly, S., Ramos-Martinez, J., and Tsimelzon, B., 2009, The effect of improved, low-frequency bandwidth in full-waveform inversion for velocity: 79th Ann. Internat. Mtg, Soc. Expl. Geophys., Expanded Abstracts, 3974−3977.

Li, Z. C., and Zhang, J. H., 2004, Seismic data processing method: The Press of University of Petroleum.

Li, G. L., Chen G., and Zhong J. Y., 2013, Analysis of geophone properties effects for land seismic data: Applied Geophysics, **6**(1), 91−101.

Sirgue, L., and Pratt, R. G., 2004, Efficient waveform inversion and imaging: A strategy for selecting temporal frequencies: Geophysics, **69**(1), 231−248.

Sun, J. H., Zhang, Y. S., Dong, J. G., and Han, Z. Y., 2012, Low frequency signal receiver technology: Petroleum Instrumenis, **26**(6), 73−76.

Tao, Z. F., Zhao, Y. L., and Ma, L., 2011, Low frequency seismic and low frequency vibrator: EGP, **21**(2), 71−76

ten Kroode, F., Bergler, S., Corsten, C., de Maag, J. W., Strijbos, F., and Tijhof, H., 2013, Broadband seismic data-The importance of low frequencies: Geophysics, **78**(2), WA3−WA14.

Whitcombe, D., Hodgson, L., 2007, Stabilizing the low frequencies: The Leading Edge, **26**(1), 66−72.

Woodburn, N., Hardwick, A., and Travis, T., 2011, Enhanced low frequency signal processing for sub-basalt imaging: 73rd EAGE Conference & Exhibition incorporating SPE EUROPEC, Vienna, Austria.

Wang, X. W., and Wang, H. Z., 2014, A research of high-resolution plane-wave decomposition based on compressed sensing: Chinese J. Geophys.(in Chinese), **57**(9), 2946−2960.

Yuan, S. Y., Wang, S. X., Luo, C. M., and He, Y. X., 2015, Simultaneous multitrace impedance inversion with transform-domain sparsity promotion: Geophysics, **80**(2), R71−R80.

Ziolkowski, A., Hanssen, P., Gatliff R., Jakubowicz, H., Dobson, A., Hampson, G., Li, X. Y., and Liu E. R., 2003, Use of low frequencies for sub-basalt imaging: Geophysical Prospecting, **51**(3), 169−182.

Zhang Jun-Hua, professor, received his B.S. in Geophysical Prospecting in 1987 and M.S. in Geophysical Exploration and Information Technology in 1995, and his Ph.D. from China University of Petroleum (East China) in 2002. Presently, he is at the School of Geosciences, China University of Petroleum (East China).